Hindawi
Wireless Communications and Mobile Computing
Volume 2022, Article ID 8172300, 10 pages
https://doi.org/10.1155/2022/8172300

Research Article

Fairness-Oriented Transmission Schemes for Multiuser MISO Broadcast Channels

Jianjian Wu,[1] **Xinyu Liu**,[2] **Chanzi Liu**,[2] **Chi-Tsun Cheng**,[3] **and Qingfeng Zhou**[1,2]

[1]*School of Computer Science and Information Engineering, Hefei University of Technology, Hefei, Anhui 230601, China*
[2]*School of Electric Engineering and Intelligentization, Dongguan University of Technology, Dongguan, Guangdong 523808, China*
[3]*Manufacturing, Materials and Mechatronics, School of Engineering, RMIT University, Melbourne, VIC 3000, Australia*

Correspondence should be addressed to Qingfeng Zhou; enqfzhou@ieee.org

Received 17 August 2022; Accepted 3 October 2022; Published 18 November 2022

Academic Editor: Jun Li

With the increasing number of Internet of Things (IoT), Industry 4.0 (I4.0), and mobile devices, it can be expected that base stations will have to serve more and more clients with a limited number of antennas. For their broadcast channels, nonorthogonal multiple access (NOMA) and blind interference alignment (BIA) are two efficient and commonly adopted transmission schemes. This paper conducts a comparison study on these techniques on a 3-user 2×1 multiple-input single-output (MISO) broadcast channel with a limited number of transmit antennas. Specifically, space-time block coding based NOMA (STBC-NOMA) and NOMA-assisted beamforming (NOMA-BF) are compared with BIA. Both perfect and imperfect successive interference cancellation (SIC) have been considered for NOMA-based schemes, and the theoretical achievable rates of all schemes have been derived. Furthermore, with a given fairness constraint among end users, the power allocation (PA) problems have been solved for cases when accurate channel state information is available at the transmitter (CSIT) as well as when only path loss information is available. Numerical results show the following: (1) none of the schemes under this study can always outperform the others under different SNR regions. (2) With imperfect SIC, NOMA-BF, and STBC-NOMA both suffer from a significant performance loss under a high SNR condition. (3) Fairness PA with only path loss information provides similar performance as that with perfect CSIT, thus partial CSIT is adequate for system or scheme designs in practice.

1. Introduction

In modern wireless communications networks, the ever-increasing demand for device mobility and connectivity makes system design challenging [1–3]. Over the years, various advanced communication solutions and technologies have been emerged to address the issues [4–6]. Furthermore, conventional wireless systems have been coupled with Artificial Intelligence (AI) techniques in response to the desire for a higher level of intelligence in future networks [7–10]. Among these techniques, multiuser access becomes challenging when the number of end users is much larger than the antennas of the base station. Several technologies have been developed to solve the problem, including beamforming (BF), interference alignment (IA), and nonorthogonal multiple access (NOMA). It is worth noting that channel state information (CSI) is a critical input parameter for enhancing performance in most wireless technologies [11, 12].

BF has been studied to improve MIMO systems' capacity and spectrum efficiency [13–15] for decades. For scenarios with base station's antenna number larger than its end user's number, BF-based methods like matched-filter-based BF, zero-forcing-based BF (ZF-BF), regularized ZF-BF [16], hybrid BF [17], and deep-learning-based BF algorithm [18] work well. However, when the transmit antenna number is less than the number of end users, the aforementioned BF-based methods start to fail or drop their performances. To tackle this problem, remedies like beamforming based on the signal-to-leakage-noise ratio (SLNR) have been proposed [19]. The common drawback is that the corresponding

interference leakage causes significant performance reductions, especially when trying to achieve a fair transmission power allocation (PA) among end users.

Unlike BF, which is mainly designed for serving a limited number of end users simultaneously, interference alignment (IA) is designed for scenarios where the end users' number is much larger than the base station's antenna number [20]. The main idea of IA is to adopt symbol extension to yield a big precoding space, then align interference signals into a small-enough subspace and use the remaining space for transmitting desired symbols. IA can be applied to manage interference under different scenarios, such as an IA algorithm for managing multitier interference in a two-tier HetNet [21], and an IA application for Coordinated Multi-Point (CoMP) systems [22]. Even with its remarkable potential, the practical implementation of IA is challenging. One of its limitations comes from the requirement of having a perfect CSIT. Fortunately, this requirement could be relaxed for broadcast channels by a so-called blind interference alignment (BIA) scheme which has been proposed in [23]. BIA is achieved by elaborately designing channel patterns over several symbol extensions, often known as "supersymbols". The channel pattern of BIA could be implemented naturally or artificially. Over the years, different BIAs have been proposed, such as a naturally implemented BIA in a homogeneous block fading system [24], an artificial BIA implementation with reconfigurable antennas in K-user SISO interference channels [25], a hybrid BIA and NOMA approach for inter-cluster interference canceling [26], a reconfigurable-antenna-based BIA with minimized mode-switching overhead [27], and a BIA implementation to maintain mode-switching fairness among end users [28].

Rather than divisions of time, frequency, or code, NOMA considers the power domain and uses the power division to distinguish end users, also known as power-domain NOMA (PD-NOMA). So, unlike orthogonal multiple access (OMA), NOMA uses the same time, frequency, and code resource to serve multiple end users and can achieve higher spectrum efficiency, user fairness, and lower system delay simultaneously. Since its appearance, it has been considered as a promising technique for resolving the multiple access issues mentioned before. Shortly, a general framework combining MIMO and NOMA has been constructed [29]. As the power domain is unrelated to the domains of time, frequency, and code, NOMA is compatible with most conventional methods to deliver multiple benefits simultaneously, like the NOMA-based power transfer and backscatter communication in [30], the NOMA-based mobile edge computing (MEC) in [31], and the NOMA-assisted UAV system in [32]. In PD-NOMA, successive interference cancellation (SIC) is the key component for decoding. In SIC, sequential decoding is applied, where signals with higher power than the desired signal are decoded first and then subtracted from received signals. Subsequently, the desired signal is decoded by regarding other signals as noise. Due to this sequential property in SIC, the decoding order influences performances in PD-NOMA and different attempts have been made to resolve the issues. In [33], it is shown that the decoding order has no effect on the achievable sum-rate in uplink PD-NOMA but may lead to unfairness among users. Considering users with a minimum rate requirement, they studied a joint user grouping, decoding order, and power control problem. In [34], a joint position, decoding order, and power allocation problem is investigated in an Unmanned Aerial Vehicle- (UAV-) based downlink NOMA. Besides, imperfect SIC has also been studied intensively. Since the recovery of each symbol with SIC depends on previous decodings, imperfect SIC causes severe residual error propagation, which makes NOMA difficult to adopt in practice. In [35], a power consumption problem in a multicell NOMA system has been studied, which evaluated the influence of imperfect SIC. In [36], the impact of imperfect SIC has been investigated in MIMO-NOMA systems when user fairness is considered. Results show that employing NOMA is not always beneficial when SIC imperfection is significant when compared with the MIMO-OMA scheme.

With the increasing popularity of IoT and I4.0 devices, the ratio between the number of end users and the number of antennas at the corresponding base station is expected to be more and more extreme, which can hardly be handled by conventional MIMO BF approaches. In contrast, IA and NOMA approaches appear to be more promising. However, to our best knowledge, their practicalities have not been extensively studied. In this paper, we study and compare three potential schemes, i.e., BIA, STBC-based NOMA, and NOMA-assisted BF, when power allocation with fairness is considered. Achievable sum-rates are derived for all schemes with the consideration of both perfect and imperfect SIC. PA problems for all schemes are solved by assuming accurate CSIT is available. PA problems for BIA and STBC-NOMA have been further studied by assuming only path loss information is available. The numerical simulation results show that the fair PA with partial channel information can achieve similar performance than that with perfect CSIT, and it also has a lower computation complexity. Among the three candidate schemes under this study, considering both the imperfect SIC and the overhead of perfect CSIT, BIA appears to be a promising candidate in practical scenarios.

2. System Model

Consider a K-user $M \times 1$ broadcast channel with $K = 3$ as shown in Figure 1, where the base station (BS) is equipped with $M = 2$ antennas, and the k-th user (Rx-k) is equipped with $N_k = 1$ antenna. Let d_k be the achievable degree-of-freedom (DoF) of the k-th user, then $d_k \leq \min(M, N_k)$. Moreover, the maximum achievable sum DoF is upper bounded by $\min(M, \sum_{k=1}^{K} N_k)$ [20]. This model is a simple example of a multiuser channel in which the end user's number is larger than the number of BS's antennas, i.e., $M < K$. In this channel, we apply a composite link model with both quasistatic Rayleigh fading and large-scale path loss considered. Then the channel matrix from BS to Rx-k is modeled as $\boldsymbol{h}_k = \boldsymbol{g}_k / \sqrt{L(l_k)}$, where $\boldsymbol{h}_k, \boldsymbol{g}_k \in \mathbb{C}^{N_k \times M}$ and $\boldsymbol{g}_k$ being a Rayleigh fading channel matrix, and l_k is the distance between BS and Rx-k. The path loss function $L(l_k)$ is given by

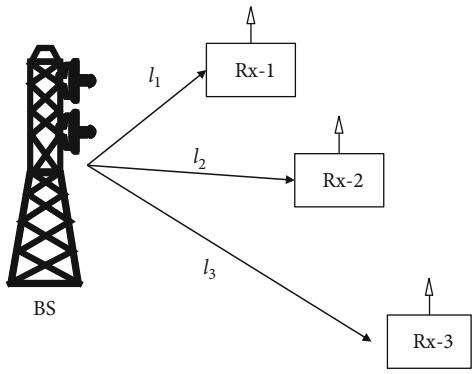

Figure 1: System model of 3-user 2×1 broadcast channel.

$$L(l_k) = \begin{cases} {l_k}^{\alpha}, & \text{if } l_k > r_0 \\ {r_0}^{\alpha}, & \text{otherwise} \end{cases}, \tag{1}$$

where $\alpha = 3$ denotes the path loss exponent [37–39] and the parameter r_0 avoids the singularity problem when l_k is very small. Without loss of generality, we assume $l_1 < l_2 < l_3$, so user-1 has the least path loss. Moreover, we suppose all channels undergo additive white Gaussian noise (AWGN) with zero-mean and variance σ^2, where the effect of noise on the communication systems can be found in [40, 41].

Denote $s_k^j \in \mathbb{C}$ as the j-th symbol transmitted to the k-th user, we assume $\mathbb{E}[|s_k^j|^2] = \rho_k P$ where ρ_k is the corresponding power allocation coefficient for user-k and P is the average transmit energy per time slot from BS.

To sever this multiuser channel, simply apply orthogonal multiaccess (OMA) schemes. However, OMA schemes, in general, have lower QoS flexibility than NOMA and IA techniques.

3. Schemes with Full CSIT

3.1. Blind Interference Alignment. The key component of BIA is the particular feasible channel patterns, also known as supersymbols. Table 1 shows the feasible channel patterns conducted by [23, 24], respectively. Without loss of generality, in this paper, we consider the reconfigurable-antenna-based BIA in [23]. In this scheme, each receiver node is assumed to be equipped with a reconfigurable antenna, which can switch its operating mode across time slots. Table 1(a) shows how the receive antennas switch their modes over a 4-slots supersymbol. In the table, we denote $\boldsymbol{h}_k(m)$ as the channel vector when the Rx-k's antenna is on the m-th mode. Here, we use three precoding matrices $[\mathbf{I}\,\mathbf{I}\,\mathbf{0}\,\mathbf{0}]^T$, $[\mathbf{I}\,\mathbf{0}\,\mathbf{I}\,\mathbf{0}]^T$ and $[\mathbf{I}\,\mathbf{0}\,\mathbf{0}\,\mathbf{I}]^T$, for user-1, user-2, and user-3, respectively.

Consider Rx-1, the received signal through 4 slots is

$$\mathbf{y}_1 = \begin{bmatrix} \boldsymbol{h}_1(1) \\ \boldsymbol{h}_1(2) \\ \mathbf{0} \\ \mathbf{0} \end{bmatrix} \begin{bmatrix} s_1^1 \\ s_1^2 \end{bmatrix} + \begin{bmatrix} \boldsymbol{h}_1(1) \\ \mathbf{0} \\ \boldsymbol{h}_1(1) \\ \mathbf{0} \end{bmatrix} \begin{bmatrix} s_2^1 \\ s_2^2 \end{bmatrix} + \begin{bmatrix} \boldsymbol{h}_1(1) \\ \mathbf{0} \\ \mathbf{0} \\ \boldsymbol{h}_1(1) \end{bmatrix} \begin{bmatrix} s_3^1 \\ s_3^2 \end{bmatrix} + \mathbf{z}_1, \tag{2}$$

where s_k^j is the j-th symbol for the k-th user and $\mathbf{z}_1$ is the AWGN vector with covariance matrix $\sigma^2\mathbf{I}$. Then, a normalized decoding matrix $\boldsymbol{U}_1 = \begin{bmatrix} 1/\sqrt{3} & 0 & -(1/\sqrt{3}) & -(1/\sqrt{3}) \\ 0 & 1 & 0 & 0 \end{bmatrix}$ is used for user-1 and thus we have

$$\boldsymbol{U}_1\boldsymbol{y}_1 = \begin{bmatrix} \left(1/\sqrt{3}\right)\boldsymbol{h}_1(1) \\ \boldsymbol{h}_1(2) \end{bmatrix} \begin{bmatrix} s_1^1 \\ s_1^2 \end{bmatrix} + \mathbf{u}_1\mathbf{z}_1, \tag{3}$$

where $\mathbf{U}_1\mathbf{z}_1$ denotes the AWGN after the postprocessing and its elements are iid noise with zero-mean and variance σ^2.

Let $\widehat{\boldsymbol{H}}_k = [(1/\sqrt{3})\boldsymbol{h}_k^T(1) \quad \boldsymbol{h}_k^T(2)]^T$, then the achievable rate for user–k is

$$R_k^{\text{BIA}} = \frac{1}{4}\mathbb{E}\left[\log\det\left(\mathbf{I} + \gamma\rho_k\widehat{\boldsymbol{H}}_k\widehat{\boldsymbol{H}}_k^{\dagger}\right)\right], \tag{4}$$

where ρ_k is the power allocation coefficient for user-k, $\gamma = P/\sigma^2$ is the transmit SNR from BS, and $\widehat{\boldsymbol{H}}_k^{\dagger}$ is the conjugate transpose of $\widehat{\boldsymbol{H}}_k$. Here, the design of one supersymbol occupying 4 time slots gives the coefficient 1/4.

Since each user's symbols are transmitted twice in a BIA supersymbol, and each supersymbol has four time slots, we have the power constraint $2(\sum_{k=1}^{K}\sum_{j=1}^{M}|s_k^j|^2) = 2MP(\sum_{k=1}^{K}\rho_k) \le 4P$, hence $\sum_{k=1}^{K}\rho_k \le 1$. Further, we consider a power allocation with max-min fairness

$$\begin{aligned} (P1) \quad & \max_{\rho_k(k\in[1,K])} \quad \min R_k^{\text{BIA}} \\ s.t. \quad & C_1 : \sum_{k=1}^{K}\rho_k \le 1, \\ & C_2 : \rho_k \ge 0. \end{aligned} \tag{5}$$

Note that BIA usually does not consider the power allocation problem since its implementation needs no CSIT or any feedback. The power allocation problem for BIA provides an upper bound and is used in the following performance comparison.

To deal with the complicated objective function in equation (5), we introduce an auxiliary variable $r \ge 0$, and equation (5) can be transformed as

$$\begin{aligned} (P2) \quad & \max_{\rho_k(k\in[1,K]),r} \quad r \\ s.t. \quad & C_1 : R_k^{\text{BIA}} \ge r, \forall k \in [1, K]. \\ & C_2 : \sum_{k=1}^{K}\rho_k \le 1, \\ & C_3 : \rho_k \ge 0, r \ge 0. \end{aligned} \tag{6}$$

Thus, problem (6) is a convex programming problem and can be solved by convex optimization tools.

3.2. STBC-Based NOMA. In downlink power-domain NOMA, signals for end users are superposed with different power allocated, then each receiver deploys successive

Table 1: Supersymbols of the 3-user 2×1 BIA

(a) 4-slots supersymbol in [23]

	Slot 1	Slot 2	Slot 3	Slot 4
User-1	$\boldsymbol{h}_1$ (1)	$\boldsymbol{h}_1$ (2)	$\boldsymbol{h}_1$ (1)	$\boldsymbol{h}_1$ (1)
User-2	$\boldsymbol{h}_2$ (1)	$\boldsymbol{h}_2$ (1)	$\boldsymbol{h}_2$ (2)	$\boldsymbol{h}_2$ (1)
User-3	$\boldsymbol{h}_3$ (1)	$\boldsymbol{h}_3$ (1)	$\boldsymbol{h}_3$ (1)	$\boldsymbol{h}_3$ (2)

(b) 4-slots supersymbol in [24]

	Slot 1	Slot 2	Slot 3	Slot 4
User-1	$\boldsymbol{h}_1$ (1)	$\boldsymbol{h}_1$ (1)	$\boldsymbol{h}_1$ (2)	$\boldsymbol{h}_1$ (2)
User-2	$\boldsymbol{h}_2$ (1)	$\boldsymbol{h}_2$ (2)	$\boldsymbol{h}_2$ (2)	$\boldsymbol{h}_2$ (2)
User-3	$\boldsymbol{h}_3$ (1)	$\boldsymbol{h}_3$ (1)	$\boldsymbol{h}_3$ (1)	$\boldsymbol{h}_3$ (2)

interference cancellation (SIC) to decode its desired signal. Unlike in BF, in NOMA, a BS can serve multiple end users simultaneously through the power-domain scheme, even though the number of transmit antennas is less than the number of end users. Further, since two transmit antennas are available, to achieve the full transmit diversity gain, we utilize the space-time block code (STBC). Specifically, we consider the Alamouti code.

The STBC-based and superposed signals at BS is given by

$$\boldsymbol{x} = \begin{bmatrix} x_1 \\ x_2 \end{bmatrix} = \begin{bmatrix} \sum_{k=1}^{K} s_k^1 \\ \sum_{k=1}^{K} s_k^2 \end{bmatrix}, \tag{7}$$

where s_k^j is the j-th symbol for the k-th user, with transmit power allocated by $\rho_k P$.

On the receiver side, for instance, the received signal at user-k is

$$\begin{bmatrix} y_k(1) \\ y_k^*(2) \end{bmatrix} = \begin{bmatrix} h_k^1 & h_k^2 \\ h_k^{2*} & -h_k^{1*} \end{bmatrix} \begin{bmatrix} x_1 \\ x_2 \end{bmatrix} + \begin{bmatrix} z_k(1) \\ z_k^*(2) \end{bmatrix}, \tag{8}$$

where $y_k(t)$ denotes the received signal of the k-th user at the t-th time/symbol slot, y^* denotes the conjugate of a complex number y, and $z_k(t)$ denotes the corresponding AWGN with zero-mean and the variance of σ^2. Note that h_k^j is the channel coefficient from the j-th transmit antenna to the k-th user. Since $l_1 < l_2 < l_3$ is assumed in our model and the decoding order of SIC depends on the channel quality, then the decoding order of three end users' signals is user-3, user-2, and user-1. For instance, user-1 needs to decode the signals for user-3 and user-2 successively and then subtract them from the superposed signal, before decoding its desired symbol.

In this paper we consider imperfect SIC, thus we denote a parameter μ as the level of residual interference because of SIC imperfection. Particularly, $\mu = 0$ implies perfect SIC, and $\mu = 1$ implies no SIC. The value of μ is influenced by the type of receivers, channel characteristics, and hardware sensibility. In practice, μ can be easily calculated at the receivers [36].

Assume $\widehat{\boldsymbol{H}}_k = \begin{bmatrix} h_k^1 & h_k^2 \\ h_k^{2*} & -h_k^{1*} \end{bmatrix}$, we have $\widehat{\boldsymbol{H}}_k \widehat{\boldsymbol{H}}_k^\dagger = \widehat{\boldsymbol{H}}_k^\dagger \widehat{\boldsymbol{H}}_k = (|h_k^1|^2 + |h_k^2|^2)\mathbf{I}$. Note that $\gamma = P/\sigma^2$ is the transmit SNR, thus the covariance matrix of the desired signal vector can be derived as

$$\mathbf{V}^k = \mathbb{E}\left[\gamma \rho_k \widehat{\boldsymbol{H}}_k \widehat{\boldsymbol{H}}_k^\dagger\right]. \tag{9}$$

Further, we can derive the covariance matrices of interference from users with decoding order larger than user-k and from residual interference due to SIC imperfection, which can be formulated, respectively, as

$$\mathbf{V}_{SIC}^{(k)} = \mathbb{E}\left[\gamma \left(\sum_{i=1}^{k-1} \rho_i\right) \widehat{\boldsymbol{H}}_k \widehat{\boldsymbol{H}}_k^\dagger\right] = \mathbb{E}\left[\gamma \rho_k^{SIC} \widehat{\boldsymbol{H}}_k \widehat{\boldsymbol{H}}_k^\dagger\right], \tag{10}$$

$$\mathbf{V}_{imp}^{(k)} = \mathbb{E}\left[\gamma \left(\mu \sum_{i=k+1}^{K} \rho_i\right) \widehat{\boldsymbol{H}}_k \widehat{\boldsymbol{H}}_k^\dagger\right] = \mathbb{E}\left[\gamma \rho_k^{imp} \widehat{\boldsymbol{H}}_k \widehat{\boldsymbol{H}}_k^\dagger\right]. \tag{11}$$

Note that $\rho_k^{SIC} = 0$ when $k = 1$ and $\rho_k^{imp} = 0$ when $k = K$.

Recall the Alamouti scheme requires 2 time slots, the achievable rate per time slot of user-k is derived as

$$\begin{aligned} R_k^{\text{S-NOMA}} &= \frac{1}{2}\mathbb{E}\left[\text{logdet}\left(\mathbf{I} + \frac{\gamma \rho_k \widehat{\boldsymbol{H}}_k \widehat{\boldsymbol{H}}_k^\dagger}{\mathbf{I} + \gamma \rho_k^{SIC} \widehat{\boldsymbol{H}}_k \widehat{\boldsymbol{H}}_k^\dagger + \gamma \rho_k^{imp} \widehat{\boldsymbol{H}}_k \widehat{\boldsymbol{H}}_k^\dagger}\right)\right] \\ &= \frac{1}{2}\mathbb{E}\left[\text{logdet}\left(\frac{\mathbf{I} + \gamma\left(\rho_k + \rho_k^{SIC} + \rho_k^{imp}\right) \widehat{\boldsymbol{H}}_k \widehat{\boldsymbol{H}}_k^\dagger}{\mathbf{I} + \gamma\left(\rho_k^{SIC} + \rho_k^{imp}\right) \widehat{\boldsymbol{H}}_k \widehat{\boldsymbol{H}}_k^\dagger}\right)\right] \\ &= \frac{1}{2}\mathbb{E}\left[\log\left(\frac{1 + \gamma\left(\rho_k + \rho_k^{SIC} + \rho_k^{imp}\right)\left(|h_k^1|^2 + |h_k^2|^2\right)}{1 + \gamma\left(\rho_k^{SIC} + \rho_k^{imp}\right)\left(|h_k^1|^2 + |h_k^2|^2\right)}\right)^2\right] \\ &= \mathbb{E}\left[\log\left(1 + \frac{\gamma \rho_k \left(|h_k^1|^2 + |h_k^2|^2\right)}{1 + \gamma\left(\rho_k^{SIC} + \rho_k^{imp}\right)\left(|h_k^1|^2 + |h_k^2|^2\right)}\right)\right] \\ &= \mathbb{E}\left[\log\left(1 + \frac{\mathscr{F}_k}{\mathscr{G}_k}\right)\right], \end{aligned} \tag{12}$$

By applying similar transformation in equation (6), the power allocation problem for STBC-based NOMA is formulated as

$$(P3) \quad \max_{\rho_k(k\in[1,K]),r} \quad r$$
$$s.t. \quad C_1 : \frac{\mathscr{F}_k}{\mathscr{G}_k} \geq r, \forall k \in [1,K], \quad (13)$$
$$C_2 : \sum_{k=1}^{K} \rho_k \leq 1,$$
$$C_3 : \rho_k \geq 0, r \geq 0.$$

Problem (13) is intractable due to the nonconvexity of C_1, but can be transformed into geometric programming (GP) [42]. Here, we introduce a variable $t = 1/r$, thus problem (13) can be transformed as

$$(P4) \quad \min_{\rho_k(k\in[1,K]),t} \quad t$$
$$s.t. \quad C_1 : \frac{\mathscr{G}_k}{\mathscr{F}_k} \leq t, \forall k \in [1,K], \quad (14)$$
$$C_2 : \sum_{k=1}^{K} \rho_k \leq 1,$$
$$C_3 : \rho_k \geq 0, t \geq 0.$$

Since $\mathscr{G}_k$ is a posynomial and $\mathscr{F}_k$ is a monomial, $\mathscr{G}_k/\mathscr{F}_k$ should be a posynomial. Then problem (14) is GP and can be solved by convex programming [42].

3.2.1. NOMA-Based Beamforming. In this scheme, we consider full CSIT and employ the conventional BF method. Note that the maximum achievable DoF in this system is 2, which is smaller than the number of end users. In this model, traditional zero-forcing-based beamforming (ZF-BF) cannot be well applied, since the whole signal space cannot provide interference-free transmission for all end users simultaneously. Other BF schemes, such as BF based on the signal-to-leakage-noise ratio (SLNR) [19], are declared to be feasible when $M < K$. However, in this model, an overloaded user causes much interference leakage, hence significant performance declines especially when considering a max-min fair power allocation. So, inspired by [43], we use a singular value decomposition- (SVD-) based BF scheme to serve some end users and use power-domain NOMA simultaneously to serve the remaining end users.

In this joint scheme, we suppose a simple NOMA pairing scheme has been adopted for user clustering. Assume that user-1 experiences the best channel and user-3 experiences the worst, then we collect user-1 and user-3 to form a NOMA pair. By the joint scheme, we use BF to cancel the intercluster interference and suppress the intracluster interference by using NOMA.

Let $s_k \in \mathbb{C}$ be the scheduled symbol for the k-th user, the the precoded signal at the BS is

$$\boldsymbol{x} = \boldsymbol{v}_1(s_1 + s_3) + \boldsymbol{v}_2 s_2, \quad (15)$$

where $\boldsymbol{v}_k \in \mathbb{C}^{M\times 1}$ denotes the transmit BF vector. By applying SVD for $\boldsymbol{h}_2$, we have $\boldsymbol{h}_2 = \boldsymbol{S}_2\boldsymbol{\Lambda}_2\boldsymbol{D}_2^H$, where $\boldsymbol{\Lambda}_2$ contains the singular values of $\boldsymbol{h}_2$. Besides, the columns of $\mathbf{S}_2$ and $\boldsymbol{D}_2$ are the left-singular vectors and right-singular vectors. We then choose a right-singular vector $\boldsymbol{v}_1$ in $\boldsymbol{D}_2$ corresponding to the zero singular value in $\boldsymbol{\Lambda}_2$. Thus $\boldsymbol{h}_2\boldsymbol{v}_1 = 0$ is achieved to eliminate interuser interference. Similarly, we can choose $\boldsymbol{v}_2$ by applying SVD of $\boldsymbol{h}_1$ and thus $\boldsymbol{h}_1\boldsymbol{v}_2 = 0$. Note that in the NOMA-based BF scheme, the channel information of user-1 is chosen for deriving v_2, so there is no interference from user-2 to user-1, but the interference leakage from user-2 to user-3 is unavoidable.

In this section, we assume $\mathbb{E}[|s_k|^2] = \rho_k P$. For user-2, interference signals due to the NOMA pair are canceled by BF, hence the SINR is

$$\mathrm{SINR}_2^{\mathrm{NOMA-BF}} = \gamma\rho_2|\boldsymbol{h}_2\boldsymbol{v}_2|^2. \quad (16)$$

For user-1, BF is used to suppress the interference from user-2. User-1 first decodes the symbols for user-3, then subtracts them to get its desired signal s_1. Considering imperfect SIC, the SINR is

$$\mathrm{SINR}_1^{\mathrm{NOMA-BF}} = \frac{\gamma\rho_1|\boldsymbol{h}_1\boldsymbol{v}_1|^2}{1 + \mu\gamma\rho_3|\boldsymbol{h}_1\boldsymbol{v}_1|^2}. \quad (17)$$

For user-3, after considering the intereference from both v_1 and v_2, the SINR is given by

$$\mathrm{SINR}_3^{\mathrm{NOMA-BF}} = \frac{\rho_3|\boldsymbol{h}_3\boldsymbol{v}_1|^2}{\rho_2|\boldsymbol{h}_3\boldsymbol{v}_2|^2 + \rho_1|\boldsymbol{h}_3\boldsymbol{v}_1|^2 + (1/\gamma)}. \quad (18)$$

Since no symbol extensions are required in NOMA-based beamforming, the average achievable rate of user-k is denoted as

$$R_k^{\mathrm{NOMA-BF}} = \mathbb{E}[\log(1 + \mathrm{SINR}_k)]. \quad (19)$$

Similarly in (6), an auxiliary variable t is introduced to formulate a max-min fairness problem as

$$(P5) \quad \min_{\rho_k(k\in[1,K]),t} \quad t$$
$$s.t. \quad C_1 : \frac{1}{\mathrm{SINR}_k^{\mathrm{NOMA-BF}}} \leq t, \forall k \in [1,K], \quad (20)$$
$$C_2 : \sum_{k=1}^{3} \rho_k \leq 1,$$
$$C_3 : \rho_k, t \geq 0,$$

where C_2 is provided to meet the transmit power constraint. Since the precoders $\boldsymbol{v}_\mathrm{k}$ have been normalized, therefore $\mathbb{E}[\mathbf{x}] = \sum_k \rho_k P \leq P$, and hence C_2 is derived.

Note that $1/\mathrm{SINR}_k^{\mathrm{NOMA-BF}}$ are posynomials, thus equation (20) is a GP problem.

4. Schemes with Partial CSIT

As shown in Sect.(III-A) and Sect.(III-B), the formulated power allocation problems require CSIT to solve. However, in practice, perfect CSIT is hard to acquire. A more general

situation is utilizing partial CSIT for power allocation, e.g., path loss information or statistical information of channels. Here, assume an LoS path loss channel model in power allocation. That is,

$$\boldsymbol{h}_k = \frac{\mathbf{1}_{N_k \times M}}{\sqrt{L(l_k)}}, \tag{21}$$

where $\mathbf{1}_{N_k \times M}$ is a $N_k \times M$ matrix with each element be 1.

Although we neglect the small-scale fading, the corresponding optimized power allocation is still useful for the optimization problem under the Rayleigh fading channel.

4.1. Power Allocation for BIA. By substituting the LoS model (21) into (4), we have the achievable rate of the k-th user in BIA expressed by

$$\begin{aligned}\dot{R}_k^{\mathrm{BIA}} &= \frac{1}{4}\log\det\left(\mathbf{I} + \rho_k \gamma l_k^{-\alpha}\begin{bmatrix}\frac{1}{\sqrt{3}}\mathbf{1}_{1,2}\\ \mathbf{1}_{1,2}\end{bmatrix}\begin{bmatrix}\frac{1}{\sqrt{3}}\mathbf{1}_{2,1} & \mathbf{1}_{2,1}\end{bmatrix}\right)\\ &= \frac{1}{4}\log\left(1 + \frac{8}{3}\rho_k \gamma l_k^{-\alpha}\right).\end{aligned} \tag{22}$$

Assume $\mathrm{sinr}_k^B = (8/3)\rho_k \gamma l_k^{-\alpha}$, the fairness power allocation problem is

$$\begin{aligned}(P6)\qquad &\max_{\rho_k(k\in[1,K]),r} \quad r\\ s.t.\quad &C_1 : \mathrm{sinr}_k^B \geq r, \forall k \in [1,K],\\ &C_2 : \textstyle\sum_{k=1}^K \rho_k \leq 1,\\ &C_3 : 0 \leq \rho_k.\end{aligned} \tag{23}$$

Note that (23) is a linear programming problem and can be easily solved by the Lagrange dual theory. By applying the Karush-Kuhn-Tucker (KKT) condition, we can get the optimal power allocation by

$$\rho_k = \frac{l_k^{\alpha}}{\sum_{i=1}^K l_i^{\alpha}}, \forall k \in [1,K] \tag{24}$$

4.2. Power Allocation for STBC-NOMA. Assuming the LoS model in (21), the covariance matrix of the desired signal vector for the k-th user in STBC-NOMA is

$$\mathbf{V}^k = 2 l_k^{-\alpha} \rho_k \gamma \mathbf{I}, \tag{25}$$

where

$$\mathbf{V}_{SIC}^{(k)} = 2 l_k^{-\alpha}\left(\sum_{i=1}^{k-1}\rho_i\right)\gamma\mathbf{I} = a^{(k)}\mathrm{I}, \tag{26}$$

$$\mathbf{V}_{imp}^{(k)} = 2 l_k^{-\alpha}\mu\left(\sum_{i=k+1}^{K}\rho_i\right)\gamma\mathbf{I} = b^{(k)}\mathbf{I}. \tag{27}$$

Thus the achievable rate is

$$R_k^{S-NOMA} = \log\left(1 + \frac{2 l_k^{-\alpha}\rho_k\gamma}{1 + a^{(k)} + b^{(k)}}\right) = \log\left(1 + \mathrm{sinr}_k^{S-NOMA}\right) \tag{28}$$

Similarly to the problem in (14), the power allocation problem can be formulated as

$$\begin{aligned}(P7)\qquad &\min_{\rho_k(k\in[1,K]),t} \quad t\\ s.t.\quad &C_1 : \frac{1}{\mathrm{sinr}_k^B} \leq t, \forall k \in [1,K],\\ &C_2 : \textstyle\sum_{k=1}^K \rho_k \leq \frac{1}{2},\\ &C_3 : \rho_k \geq 0, t \geq 0,\end{aligned} \tag{29}$$

which is a GP problem.

5. Simulation Results and Discussion

In this section, all the schemes mentioned previously are compared via numerical simulation. Suppose $l_1 = 4$, $l_2 = 5$, and $l_3 = 6$. Since in this paper, we consider end users with different distances to the BS, and the channel quality is related directly to the distance, we adopt the NOMA clustering scheme according to the distance. For example, since $l_1 < l_2 < l_3$, the decoding order in SIC of STBC-NOMA will be user-3, user-2, and then user-1, while in NOMA-BF, user-3 will be paired with user-1.

5.1. Schemes with Perfect CSIT. Figure 2 shows the ergodic achievable sum-rate for the three schemes with perfect SIC in linear scale and logarithmic scale, respectively. Note that in this section, perfect CSIT is considered for power allocation. The figures show that, under the low and medium SNR scenarios, the STBC-NOMA scheme outperforms other schemes, while BIA is better than NOMA-BF. The reasons are as follows: (1) the rate enhancement yielded by the diversity gain of STBC-NOMA is larger than the contributions of multiplexing gain that the other two schemes obtain, (2) BIA sacrifices some DoF for its fairness among three end users, (3) In NOMA-BF, because of the fairness-oriented max-min rate objective, the user with the worst channel state is allocated with much more power, which reduces the sum-rate at the low-SNR scenario.

Under the high SNR scenario, STBC-NOMA performs the worst because it offers no multiplexing gain. By contrast, NOMA-BF outperforms the other two schemes. This can be explained by the DoF/multiplexing-gain difference. In the system model considered, the sum DoF achieved by NOMA-BF is 2, the achievable sum DoF of BIA is 3/2, and STBC-NOMA only has a sum DoF 1. Interestingly, applying

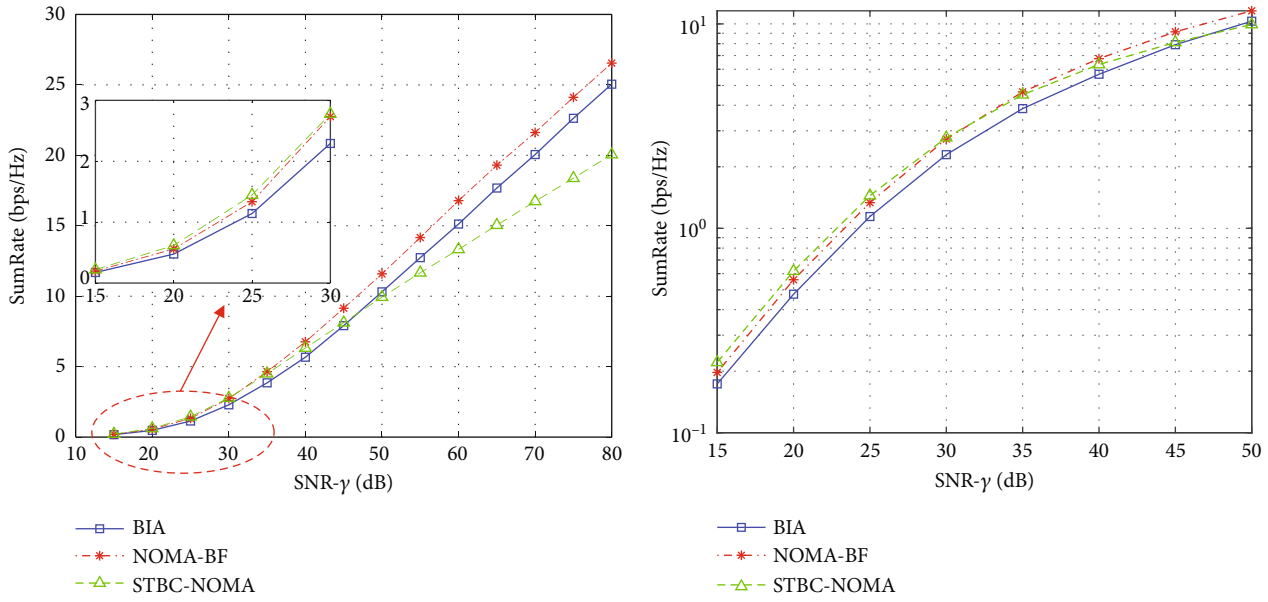

(a) Normal figure (b) Logy figure

Figure 2: Sum-rate comparison with perfect SIC (normal graph).

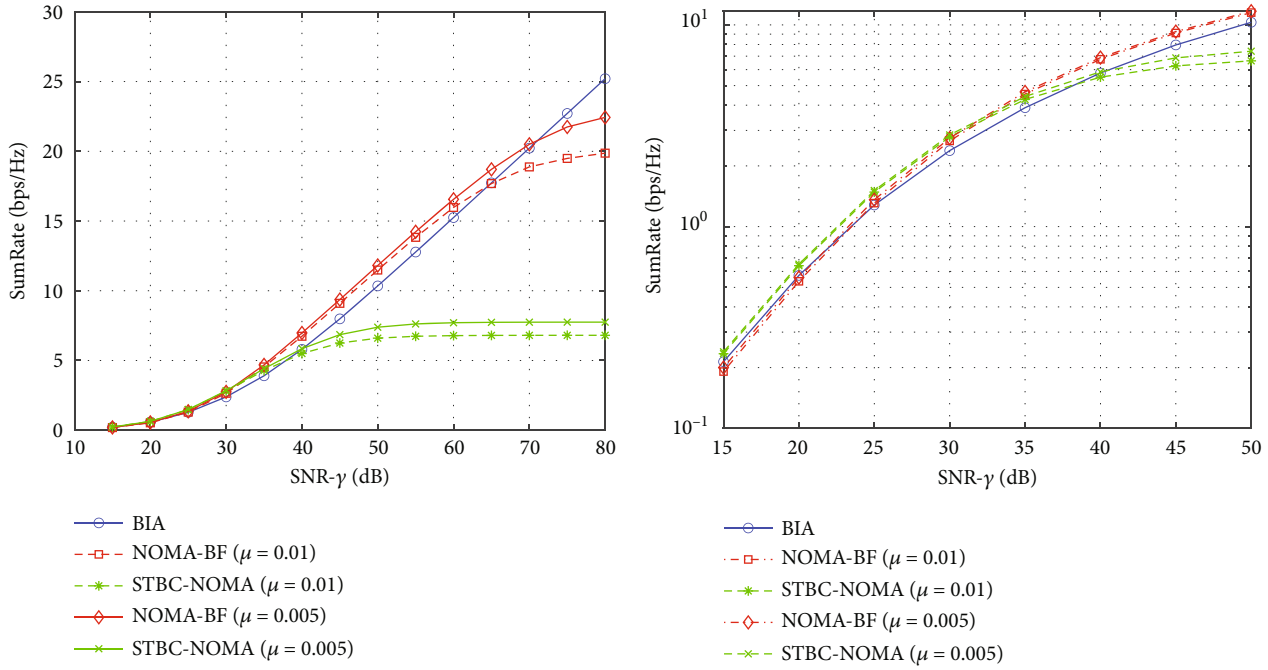

(a) Normal figure (b) Logy figure

Figure 3: Sum-rate comparison with imperfect SIC.

PA with perfect CSIT, BIA can deliver decent performances under both low and high SNR scenarios.

Figure 3 shows the ergodic achievable sum-rate consider imperfect SIC in NOMA-based schemes. From the figure we observe the following: (1) compared with systems with perfect SIC, there is performance loss on NOMA-BF and STBC-NOMA with imperfect SIC under the high SNR scenarios. The reason is that residual interference on SIC is proportional to SNR, thus leading to a significant performance loss on the sum-rate under high SNR. (2) The imperfection of SIC causes much performance loss on STBC-NOMA than on NOMA-BF. This can be explained by the different levels of residual interference in the two schemes. In NOMA-BF, only two users are clustered as a NOMA pair and apply SIC for intercluster interference cancellation. While in STBC-NOMA, all users are clustered and SIC is required for

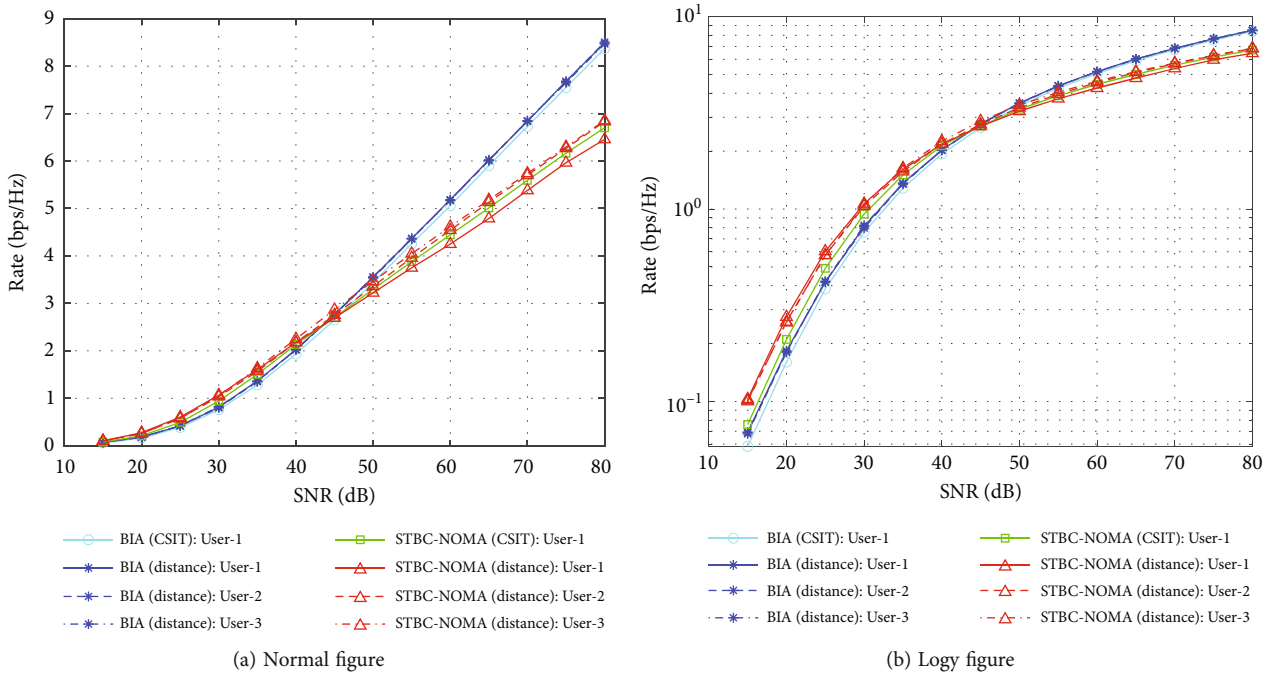

(a) Normal figure (b) Logy figure

Figure 4: PA with CSIT vs. PA with distance (perfect SIC).

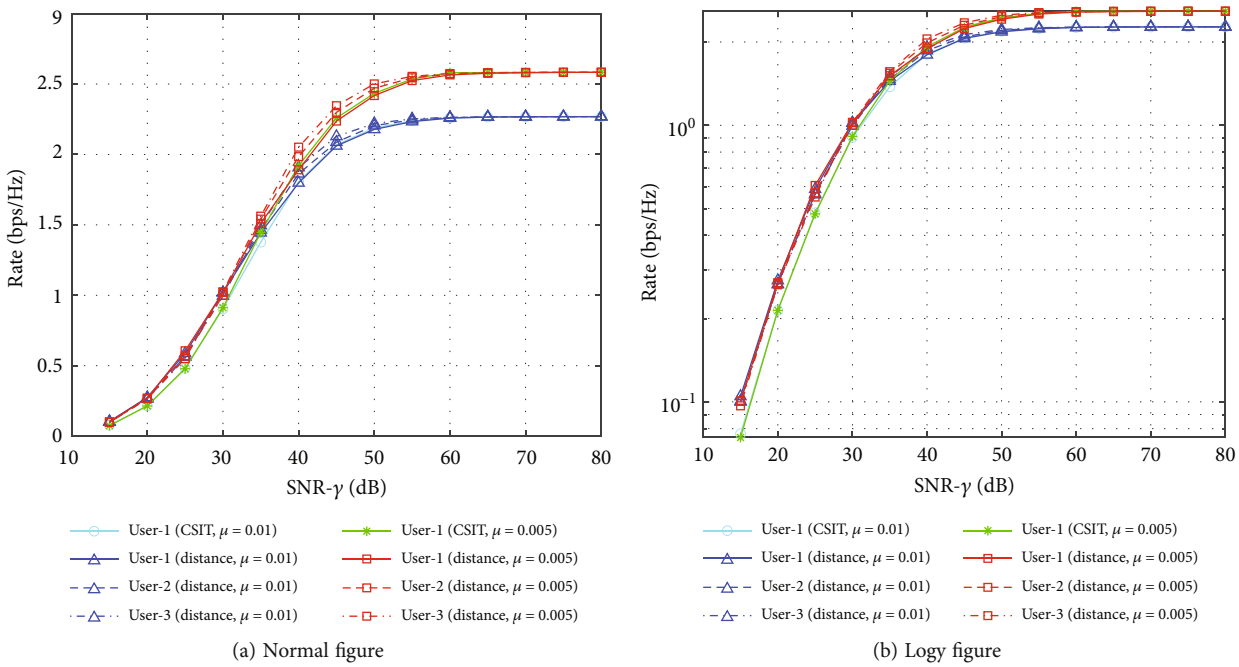

(a) Normal figure (b) Logy figure

Figure 5: PA with CSIT vs. PA with distance (in STBC-NOMA with imperfect SIC).

canceling interference among all users. (3) Under low SNR scenarios, STBC-NOMA achieves the highest sum-rate as indicated in Figure 2.

5.2. Schemes with Partial CSIT. In this section, PA considering only path loss information is compared with PA considering perfect CSIT in BIA and STBC-NOMA. Note that NOMA-BF is not considered in this section, because with only path loss information available, the precoder in NOMA-BF cannot be fully functional. Since PA with perfect CSIT can yield fair rates among users, for simplicity, we only chose user-1 considering perfect CSIT for comparison in this section.

In Figure 4, PA with perfect CSIT and with only distance information available are compared, with perfect SIC considered in NOMA. From the figure, we observe that the proposed PA with only distance information available has unequal ergodic rates among users, especially in the high SNR region. However, its performance is acceptable since

the absence of accurate CSIT and low computation complexity. The performance of BIA with perfect CSIT is very close to that of BIA with path loss information only.

Figure 5 compares the PA with perfect CSIT and with only distance information available in STBC-NOMA. In the medium SNR region, PA with only distance available achieves unequal rates among users. However, as SNR increases, equal rates among users are achieved by considering only distance information, which is the same as performance when considering accurate CSIT. The reason is that imperfect SIC provides the same rate constraint in high SNR region for each user, thus users achieve equal rates as SNR increases. Results presented in Figure 5 show that in the high SNR region, it is possible to achieve max-min fairness optimization with only distance information available when imperfect SIC is considered.

6. Conclusion

In this paper, we consider scenarios when the number of BS transmit antennas is less than the number of end users. Three feasible schemes have been investigated, i.e., BIA, STBC-NOMA, and NOMA-BF. Under PA of a max-min fairness objective, the sum-rates of the three schemes have been derived with the consideration of both perfect and imperfect SIC. Then, the formulated PA problems are solved assuming perfect CSIT is available as well as assuming only path loss information is available. Numerical simulations show that partial channel information is adequate, which can be used as a criterion in system or scheme designs. Outcomes of this study serve as guidelines for system integrators to pick the best approach for their systems. The formulations also serve as benchmarks and an evaluation framework for up-and-coming designs. For future research, different constraints/objectives can be considered in the PA. Nevertheless, the benefits of integrating NOMA and BIA should be further investigated.

Data Availability

No underlying data was collected or produced in this study.

Conflicts of Interest

The authors declare that they have no conflicts of interest.

Acknowledgments

This work was supported in part by NSFC under Grant 61971138, in part by the Science and Technology Planning Project of Guangdong Province under Grant 2016B010108002, in part by Guangdong Higher Education Innovation Project under Grant 2020ZDZX3047, and in part by the Applied Basic Research Project of Guangdong Province under Grant No. 2019A1515111149.

References

[1] X. Lai, Y. Deng, G. K. Karagiannidis, and A. Nallanathan, "Secure mobile edge computing networks in the presence of multiple eavesdroppers," *IEEE Transactions on Communications*, vol. 70, no. 1, pp. 500–513, 2022.

[2] X. Lai, J. Xia, L. Fan, T. Q. Duong, and A. Nallanathan, "Outdated access point selection for mobile edge computing with cochannel interference," *IEEE Transactions on Vehicular Technology*, vol. 71, no. 7, pp. 7445–7455, 2022.

[3] L. He, K. He, L. Fan, X. Lei, A. Nallanathan, and G. K. Karagiannidis, "Toward optimally efficient search with deep learning for large-scale MIMO systems," *IEEE Transactions on Communications*, vol. 70, no. 5, pp. 3157–3168, 2022.

[4] J. Lu and M. Tang, "Performance analysis for IRS-assisted MEC networks with unit selection," *Physical Communication*, vol. 52, article 101869, 2022.

[5] R. Zhao and M. Tang, "Impact of direct links on intelligent reflect surface-aided MEC networks," *Physical Communication*, vol. 50, article 101905, 2022.

[6] L. Chen, "Physical-layer security on mobile edge computing for emerging cyber physical systems," *Computer Communications*, vol. 194, pp. 180–188, 2022.

[7] Y. Guo, R. Zhao, S. Lai, L. Fan, X. Lei, and G. K. Karagiannidis, "Distributed machine learning for multiuser mobile edge computing systems," *IEEE Journal of Selected Topics in Signal Processing*, vol. 16, no. 3, pp. 460–473, 2022.

[8] L. Zhang and C. Gao, "Deep reinforcement learning based IRS-assisted mobile edge computing under physical-layer security," *Physical Communication*, vol. 51, no. 1, article 101896, 2022.

[9] L. Zhang, W. Zhou, J. Xia et al., "DQN-based mobile edge computing for smart internet of vehicle," *EURASIP Journal on Advances in Signal Processing*, vol. 2022, 45 pages, 2022.

[10] S. Tang, L. Chen, K. He, J. Xia, L. Fan, and A. Nallanathan, "Computational intelligence and deep learning for next-generation edge-enabled industrial IoT," *IEEE Transactions on Network Science and Engineering*, vol. 9, no. 3, pp. 1–13, 2022.

[11] S. Tang, "Dilated convolution based CSI feedback compression for massive MIMO systems," *IEEE Transactions on Vehicular Technology*, vol. 71, no. 5, pp. 211–216, 2022.

[12] Y. Wu and C. Gao, "Task offloading for vehicular edge computing with imperfect CSI: a deep reinforcement approach," *Physical Communication*, vol. 55, no. 1, article 101867, 2022.

[13] Q. H. Spencer, A. L. Swindlehurst, and M. Haardt, "Zero-Forcing methods for downlink spatial multiplexing in multiuser MIMO channels," *IEEE Transactions on Signal Processing*, vol. 52, no. 2, pp. 461–471, 2004.

[14] E. Björnson, M. Bengtsson, and B. Ottersten, "Optimal multiuser transmit beamforming: a difficult problem with a simple solution structure [lecture notes]," *IEEE Signal Processing Magazine*, vol. 31, no. 4, pp. 142–148, 2014.

[15] S. Ali, M. Sohail, S. B. H. Shah et al., "New trends and advancement in next generation mobile wireless communication (6G): a survey," *Wireless Communications and Mobile Computing*, vol. 2021, Article ID 9614520, 14 pages, 2021.

[16] N. Fatema, G. Hua, Y. Xiang, D. Peng, and I. Natgunanathan, "Massive MIMO linear precoding: a survey," *IEEE Systems Journal*, vol. 12, no. 4, pp. 3920–3931, 2017.

[17] I. Ahmed, H. Khammari, A. Shahid et al., "A survey on hybrid beamforming techniques in 5G: architecture and system model perspectives," *IEEE Communications Surveys & Tutorials*, vol. 20, no. 4, pp. 3060–3097, 2018.

[18] H. Huang, Y. Peng, J. Yang, W. Xia, and G. Gui, "Fast beamforming design via deep learning," *IEEE Transactions on Vehicular Technology*, vol. 69, no. 1, pp. 1065–1069, 2019.

[19] M. Sadek, A. Tarighat, and A. H. Sayed, "A leakage-based precoding scheme for downlink multi-user MIMO channels," *IEEE Transactions on Wireless Communications*, vol. 6, no. 5, pp. 1711–1721, 2007.

[20] C. S. Vaze and M. K. Varanasi, "The degrees of freedom region of the two-user MIMO broadcast channel with delayed CSIT," in *2011 IEEE International Symposium on Information Theory Proceedings*, pp. 199–203, St. Petersburg, Russia, 2011.

[21] C. Wang, D. Deng, L. Xu, W. Wang, and F. Gao, "Joint interference alignment and power control for dense networks via deep reinforcement learning," *IEEE Wireless Communications Letters*, vol. 10, no. 5, pp. 966–970, 2021.

[22] Z. Li, J. Chen, L. Zhen, S. Cui, K. G. Shin, and J. Liu, "Coordinated multi-point transmissions based on interference alignment and neutralization," *IEEE Transactions on Wireless Communications*, vol. 18, no. 7, pp. 3347–3365, 2019.

[23] T. Gou, C. Wang, and S. A. Jafar, "Aiming perfectly in the dark-blind interference alignment through staggered antenna switching," *IEEE Transactions on Signal Processing*, vol. 59, no. 6, pp. 2734–2744, 2011.

[24] Q. F. Zhou, Q. Zhang, and F. C. Lau, "Diophantine approach to blind interference alignment of homogeneous K-user 2x1 MISO broadcast channels," *IEEE Journal on Selected Areas in Communications*, vol. 31, no. 10, pp. 2141–2153, 2013.

[25] M. Johnny and M. R. Aref, "BIA for the k-user interference channel using reconfigurable antenna at receivers," *IEEE Transactions on Information Theory*, vol. 66, no. 4, pp. 2184–2197, 2019.

[26] M. Morales-Céspedes, O. A. Dobre, and A. Garca-Armada, "Semi-blind interference aligned NOMA for downlink MU-MISO systems," *IEEE Transactions on Communications*, vol. 68, no. 3, pp. 1852–1865, 2019.

[27] Q. F. Zhou, A. Huang, M. Peng, F. Qu, and L. Fan, "On the mode switching of reconfigurable-antenna-based blind interference alignment," *IEEE Transactions on Vehicular Technology*, vol. 66, no. 8, pp. 6958–6968, 2017.

[28] J. Wu, X. Liu, C. Qu, C.-T. Cheng, and Q. Zhou, "Balanced-switching-oriented blind interference-alignment scheme for 2-user MISO interference channel," *IEEE Communications Letters*, vol. 24, no. 10, pp. 2324–2328, 2020.

[29] Z. Ding, R. Schober, and H. V. Poor, "A general MIMO framework for NOMA downlink and uplink transmission based on signal alignment," *IEEE Transactions on Wireless Communications*, vol. 15, no. 6, pp. 4438–4454, 2016.

[30] Z. Ding, "Harvesting devices' heterogeneous energy profiles and QoS requirements in IoT: WPT-NOMA vs BAC-NOMA," *IEEE Transactions on Communications*, vol. 69, no. 5, pp. 2837–2850, 2021.

[31] P. Lai, Q. He, G. Cui et al., "Cost-effective user allocation in 5G NOMA-based mobile edge computing systems," *IEEE Transactions on Mobile Computing*, p. 1, 2021.

[32] Y. Dai, Z. Liang, L. Lyu, and B. Lin, "Deep reinforcement learning-based UAV data collection and offloading in NOMA-enabled marine IoT systems," *Wireless Communications and Mobile Computing*, vol. 2022, Article ID 8805416, 13 pages, 2022.

[33] J. Zhang, L. Zhu, Z. Xiao, X. Cao, D. O. Wu, and X.-G. Xia, "Optimal and sub-optimal uplink NOMA: joint user grouping, decoding order, and power control," *IEEE Wireless Communications Letters*, vol. 9, no. 2, pp. 254–257, 2020.

[34] D. Hu, Q. Zhang, Q. Li, and J. Qin, "Joint position, decoding order, and power allocation optimization in UAV-based NOMA downlink communications," *IEEE Systems Journal*, vol. 14, no. 2, pp. 2949–2960, 2020.

[35] M. Zeng, W. Hao, O. A. Dobre, Z. Ding, and H. V. Poor, "Power minimization for multi-cell uplink NOMA with imperfect SIC," *IEEE Wireless Communications Letters*, vol. 9, no. 12, pp. 2030–2034, 2020.

[36] A. S. de Sena, F. R. M. Lima, D. B. da Costa et al., "Massive MIMO-NOMA networks with imperfect SIC: design and fairness enhancement," *IEEE Transactions on Wireless Communications*, vol. 19, no. 9, pp. 6100–6115, 2020.

[37] J. Lu, L. Chen, J. Xia et al., "Analytical offloading design for mobile edge computing based smart internet of vehicle," *EURASIP Journal on Advances in Signal Processing*, vol. 2022, no. 1, p. 10, 2022.

[38] R. Zhao and M. Tang, "Profit maximization in cache-aided intelligent computing networks," *Physical Communication*, vol. 99, pp. 1–10, 2022.

[39] S. Tang and X. Lei, "Collaborative cache-aided relaying networks: performance evaluation and system optimization," *IEEE Journal on Selected Areas in Communications*, vol. 99, pp. 1–12, 2022.

[40] L. Chen, R. Zhao, K. He, Z. Zhao, and L. Fan, "Intelligent ubiquitous computing for future UAV-enabled MEC network systems," *Cluster Computing*, vol. 25, pp. 1–11, 2021.

[41] K. He, L. He, L. Fan, X. Lei, Y. Deng, and G. K. Karagiannidis, "Efficient memory-bounded optimal detection for GSM-MIMO systems," *IEEE Transactions on Communications*, vol. 70, no. 7, pp. 4359–4372, 2022.

[42] M. Chiang, "Geometric programming for communication systems," *Foundations and Trends® in Communications and Information Theory*, vol. 2, no. 1–2, pp. 1–154, 2005.

[43] B. Kimy, S. Lim, H. Kim et al., "Non-orthogonal multiple access in a downlink multiuser beamforming system," in *MILCOM 2013-2013 IEEE Military Communications Conference*, pp. 1278–1283, San Diego, CA, USA, 2013.